**Electronic Supplementary Information (ESI)**

# Solution blending preparation of polycarbonate/graphene composite: boosting the mechanical and electrical properties

Emanuele Lago,[a,b] Peter S. Toth,[a*] Giammarino Pugliese,[c] Vittorio Pellegrini,[a] and Francesco Bonaccorso[a*]

[a]*Istituto Italiano di Tecnologia, Graphene Labs, Via Morego 30, 16163 Genova, Italy*
[b]*Dipartimento di Chimica e Chimica Industriale, Università di Genova, Via Dodecaneso 31, 16146 Genova, Italy*
[c]*Istituto Italiano di Tecnologia, Nanochemistry Department, Via Morego 30, 16163 Genova, Italy*
*peter.toth@iit.it, francesco.bonaccorso@iit.it*

**Contents:** The additional results and discussion presented in the Supporting Information include the Raman spectroscopy results and statistical analyses obtained investigating single- and few-layer graphene flakes dispersion in 1,3-dioxolane, and the mechanical characterization data of the polycarbonate/graphene composites summarized in a table.

## Raman characterization of SLG/FLG flakes dispersion in 1.3-dioxolane

Figure S1 shows the Raman spectroscopy results obtained investigating graphene dispersion in 1,3-dioxolane, where a representative Raman spectrum is depicted in Fig. S1a. The Raman fingerprints of graphene are the G (~1580cm$^{-1}$) and 2D (~2700cm$^{-1}$) peaks.[1–4] If graphene flakes have defects, a D peak (~1350cm$^{-1}$) also appears.[1–4] The G peak corresponds to the $E_{2g}$ phonon at the Brillouin zone center.[2] The D peak is due to the breathing modes of $sp^2$ rings and requires defects for its activation, the 2D peak is the second order of the D peak and is always visible, even without the presence of defects.[5,6] Statistical analysis shows 2D peak position (Pos(2D)) (Fig. S1b) in the 2688 – 2700 cm$^{-1}$ range. The analysis of 2D peak in position, width (full width at half maximum, FWHM, Fig. S1c) and intensity (respect to the G peak, $I_{2D}/I_G$, Fig. S1d), gives information about the number of layers of the graphene flakes.[1–3] The FWHM (2D) is in average ~70 cm$^{-1}$, while the $I_{2D}/I_G$ ratio is higher than 0.5, which represents the reference value of graphite.[1] These results suggest that the dispersion is composed by a combination of both single- (SLG) and few-layer graphene (FLG) flakes,[3,7] in agreement with the atomic force microscopy (AFM) data reported (see Fig. 2d in main text). Raman spectroscopy allows also to provide indication about the nature of defects in the graphene flakes.[1,2,7] In fact, by combining the $I_D/I_G$ ratio with FWHM(G) allows us to discriminate between disorder localized at the edges and disorder in the bulk. In the latter case, a higher I(D)/I(G) would correspond to higher FWHM(G). The I(D)/I(G) ratio is in the range 0.6 – 1.6 (Fig S1e), but the lack of correlation between I(D)/I(G) and FWHM(G) (Fig. S1f) proves that the major contribution to the D peak comes from the sample edges (see Fig. 2 in main text) rather than to the presence of structural defects.[5,7] Moreover, in the high-defect concentration regime FWHM(G) and FWHM(D′) become broader and eventually merge into a single band.[5,7]

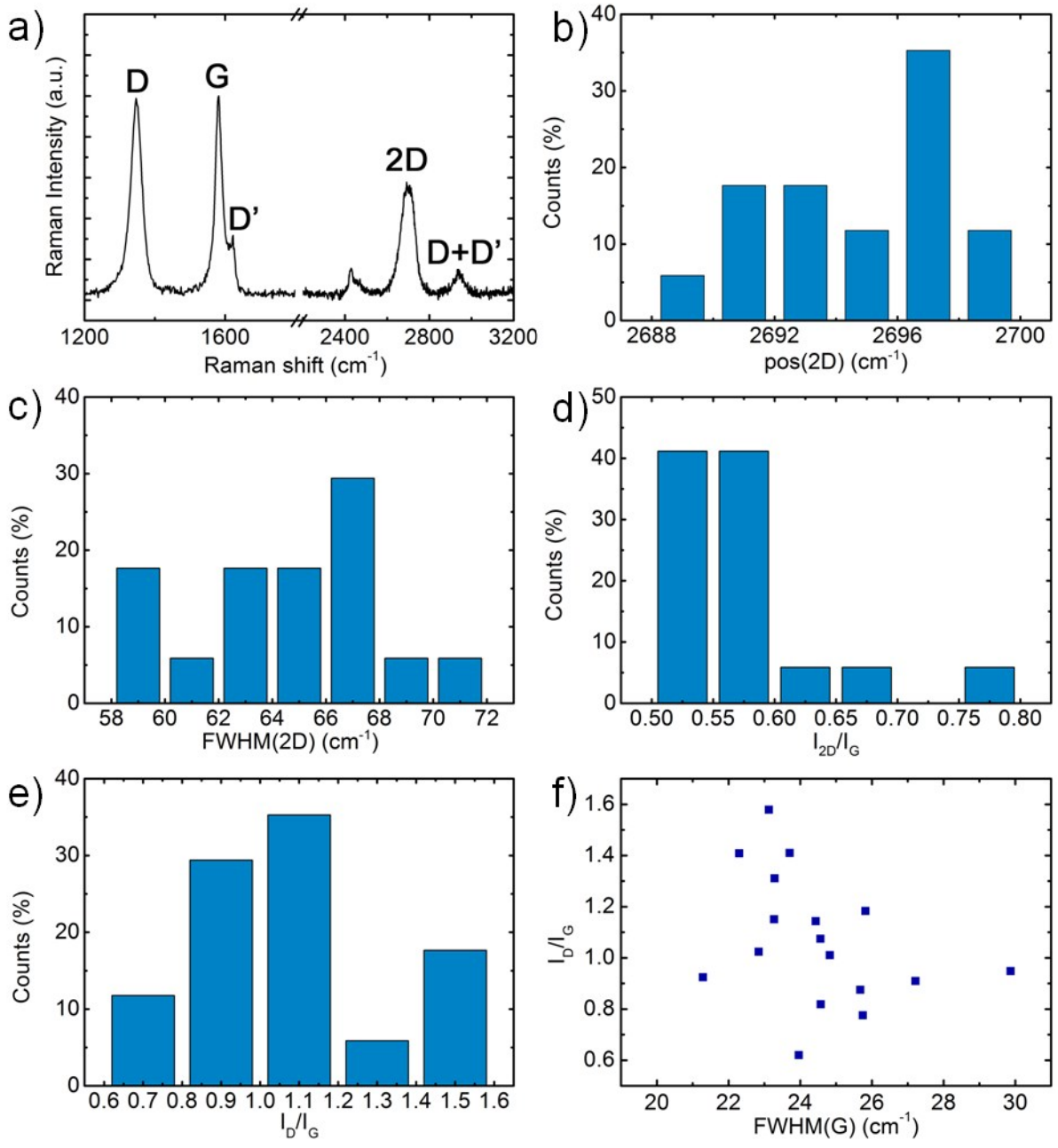


**Figure S1.** (a) Representative Raman spectrum of graphene flakes dispersed in 1-3 dioxolane. (b – f) Statistic analysis on the acquired Raman spectra: (b) pos(2D), (c) FWHM(2D), (d) $I_{2D}/I_G$, (e) $I_D/I_G$, and (f) $I_D/I_G$ as a function of FWHM(G).

## The mechanical characterization data of polycarbonate/graphene composites

The full mechanical characterization data are summarized in Table S1. The increments in mechanical properties are stated as $\Delta E$, $\Delta\sigma_Y$, and $\Delta\sigma_u$.

**Table S1.** Summary of mechanical properties of polycarbonate/graphene composite.

| SLG/FLG content | E | error E | $\Delta E$ | $\sigma_Y$ | error $\sigma_Y$ | $\Delta\sigma_Y$ | $\sigma_u$ | error $\sigma_u$ | $\Delta\sigma_u$ |
|---|---|---|---|---|---|---|---|---|---|
| wt% | MPa | MPa | % | MPa | MPa | % | MPa | MPa | % |
| 0.00 | 1151 | 44 | — | 47.9 | 2.9 | — | 55.2 | 3.4 | — |
| 0.01 | 1273 | 62 | 10.6 | 47.8 | 2.1 | -0.2 | 55.9 | 2.5 | 1.3 |
| 0.05 | 1359 | 51 | 18.1 | 48.5 | 2.4 | 1.3 | 56.2 | 3.8 | 1.8 |
| 0.10 | 1371 | 48 | 19.1 | 49.4 | 3.5 | 3.0 | 55.6 | 6.0 | 0.7 |
| 0.50 | 1403 | 34 | 21.9 | 50.8 | 1.0 | 6.0 | 60.1 | 0.9 | 8.9 |
| 1.00 | 1455 | 28 | 26.4 | 50.3 | 1.5 | 4.9 | 60.0 | 1.1 | 8.8 |
| 1.50 | 1353 | 31 | 17.6 | 51.5 | 0.2 | 7.4 | 59.3 | 1.4 | 7.6 |
| 2.00 | 1226 | 54 | 6.5 | 50.5 | 0.4 | 5.4 | 57.3 | 2.4 | 4.0 |
| 2.50 | 1353 | 69 | 17.4 | 51.6 | 1.9 | 7.4 | 60.8 | 0.2 | 10.3 |
| 3.00 | 1345 | 46 | 16.8 | 50.7 | 1.7 | 5.8 | 58.5 | 1.1 | 6.1 |

## References


1 A. C. Ferrari, J. C. Meyer, V. Scardaci, C. Casiraghi, M. Lazzeri, F. Mauri, S. Piscanec, D. Jiang, K. S. Novoselov, S. Roth and A. K. Geim, *Phys. Rev. Lett.*, 2006, **97**, 187401.

2 A. C. Ferrari and D. M. Basko, *Nat. Nanotechnol.*, 2013, **8**, 235–46.

3 F. Bonaccorso, P. H. Tan and A. C. Ferrari, *ACS Nano*, 2013, **7**, 1838–1844.

4 A. C. Ferrari, *Solid State Commun.*, 2007, **143**, 47–57.

5 A. C. Ferrari and J. Robertson, *Phys. Rev. B*, 2001, **64**, 075414.

6 A. C. Ferrari and J. Robertson, *Phys. Rev. B*, 2000, **61**, 14095–14107.

7 Y. Hernandez, V. Nicolosi, M. Lotya, F. M. Blighe, Z. Sun, S. De, I. T. McGovern, B. Holland, M. Byrne, Y. K. Gun'Ko, J. J. Boland, P. Niraj, G. Duesberg, S. Krishnamurthy, R. Goodhue, J. Hutchison, V. Scardaci, A. C. Ferrari and J. N. Coleman, *Nat. Nanotechnol.*, 2008, **3**, 563–8.